

Longitudinal and Hall conductances in model alkali fullerenes A_3C_{60}

David G. Steffen and Martin P. Gelfand

Department of Physics, Colorado State University, Fort Collins, Colorado 80523-1875, USA

(Received 10 October 2003; revised manuscript received 19 December 2003; published 17 March 2004)

We have calculated the low-temperature, low-field longitudinal and transverse conductivities for various tight-binding models intended to represent the conduction band in A_3C_{60} compounds, by directly applying the Kubo-Greenwood formula to finite clusters. It turns out that the “universal” dependence of Hall coefficient on lattice constant found for K_3C_{60} and Rb_3C_{60} [L. Lu *et al.*, Phys. Rev. Lett. **74**, 1637 (1995)] *cannot* be accounted for by appealing to two types of disorder, one of which (merohedral disorder) has an energy scale that varies strongly with lattice constant and another of which (that we model as Anderson disorder) does not. The calculations also reveal enormous violations of Matthiessen’s rule: it is even possible to decrease the resistivity by introducing merohedral disorder into a system which had only Anderson disorder.

DOI: 10.1103/PhysRevB.69.115109

PACS number(s): 72.80.Rj, 72.10.–d

I. INTRODUCTION

The discovery^{1–3} of metallicity and remarkably high-temperature superconductivity in the A_3C_{60} family of alkali-doped C_{60} solids (with $A=K, Rb$, or in part Cs) was followed in fairly short order by the emergence of a widespread conventional wisdom regarding the low-energy normal-state electronic properties of these compounds. Electronic structure calculations based on density-functional methods (see, for example, Refs. 4 and 5) indicated that a narrow conduction band was derived almost exclusively from the lowest unoccupied C_{60} molecular orbitals, the triply degenerate t_{1u} orbitals, which became half filled upon the addition of three alkali-metal atoms per molecule. The results of such calculations were largely consistent with those from the simpler extended Hückel theory approach.⁶

As far as low-energy electronic properties were concerned, the various compounds in the family differed only in the width of the conduction band and thus the density of states at E_F , which in turn was controlled by the lattice spacing a . This picture was consistent with a variety of striking experimental results, particularly the almost “universal” plot of superconducting transition temperature T_c versus a , varying a by changing both cation species and pressure.

It also became evident early on that even the best samples of K_3C_{60} (Ref. 7) and Rb_3C_{60} (Ref. 8) were not perfect crystals. In these materials the hexagonal faces of the molecules point in (111) directions so as to maximize the volume of the tetrahedral interstices, and there are two orientations, related by $\pi/2$ rotation about a twofold axis, which accomplish this. These two orientations appeared to have equal populations and no long-range order was evident; this peculiar type of restricted orientational disorder was denoted “merohedral” disorder. It was pointed out by Gelfand and Lu⁹ that such disorder alone, if the orientations were strictly uncorrelated, could render these materials dirty metals.

Much of the experimental data produced during the first few years of intense study of the A_3C_{60} compounds could be readily accounted for by the ideas mentioned above. However, they are not sufficient to account for all details of normal-state electronic transport.

If one takes for granted the results of the density-

functional calculations, uncorrelated merohedral disorder alone, as assumed in Ref. 10, cannot account for the different residual resistivities determined for K_3C_{60} ($\rho_0=180 \pm 60 \mu\Omega \text{ cm}$) and Rb_3C_{60} ($\rho_0=570 \pm 210 \mu\Omega \text{ cm}$),¹¹ which should be compared with the calculated $\rho_0=300 \pm 15 \mu\Omega \text{ cm}$ for uncorrelated merohedral disorder, independent of a . There would seem to be substantial orientational correlations in at least K_3C_{60} and quite possibly an additional scattering mechanism which has a strength that does not scale with the bandwidth, such as potential scattering due to alkali vacancies,¹² which could lead to a larger ρ_0 for larger a . (A cautionary note regarding the experimental ρ_0 values quoted above is in order: these are not from direct measurements of the resistivity, and some of the assumptions that go into those values may be in error. However, direct resistivity measurements on crystals¹³ do suggest that ρ_0 for Rb_3C_{60} is greater than that for K_3C_{60} by a factor of about 1.6, although sample inhomogeneity makes it impossible to obtain reliable absolute values.)

The present work was motivated by a remarkable experimental finding by Lu *et al.*,¹³ namely, that the low-field Hall coefficient R_H in high quality samples of K_3C_{60} and Rb_3C_{60} appeared to vary “universally” with lattice constant, reminiscent of T_c . (An earlier study of K_3C_{60} thin films by Palstra *et al.*¹⁴ led to data consistent with theirs.) Unlike the T_c studies, a was varied by changing the *temperature* as well as the chemical composition. If one makes the assumption that R_H is dominated by zero-temperature physics, as is usually the case in metals, then their finding seems on the face of it to be yet another confirmation of the standard picture of the electronic structure, in which the lattice constant is the key control parameter for electronic properties of A_3C_{60} compounds because it in turn sets the conduction bandwidth.

Let us for the moment take the universality of R_H versus a for granted, and with it the assumption that R_H reflects low-temperature properties. (Further support for that assumption is offered by the Boltzmann equation analysis of Schulz and Allen.¹⁵) Then there is something rather odd about the data. According to the conventional wisdom the only thing that can change at low temperature as a function of a is the strength of (some kinds of) disorder relative to

the bandwidth, but Lu *et al.* find R_H varying from -2.9×10^{-9} m/C at $a = 1.416$ nm (K_3C_{60} at 60 K) to 1.0×10^{-9} m/C at $a = 1.444$ nm (Rb_3C_{60} at 300 K), with a sign change at $a = 1.435$ nm. This sort of variation in R_H for a metal just as a function of disorder is, as far as we are aware, unprecedented. Schulz and Allen also note that the dependence of R_H on underlying scattering mechanisms should be weak in a generic metal. Lu *et al.* suggest that the interplay of merohedral disorder with other types of disorder (not described in detail, but assumed to have a strength roughly independent of a) could be responsible for the variation of R_H , and offer an argument based on Ong's scattering-length-surface construction applied to supercell Fermi surfaces to justify it. We found their argument less than convincing, and felt it was worth trying to confirm their suggestion by a direct calculation. That provided the initial motivation for the calculations to be presented below. In the end, the calculations suggest that something entirely different must be responsible for the variation of R_H .

The plan of the paper is as follows. The tight-binding models used to represent conduction-band states are described in Sec. II, followed by a discussion of the method applied to estimate the longitudinal and low-field transverse conductivities for these models in Sec. III. Results from an extensive set of numerical calculations are discussed in Sec. IV, and conclusions are presented in Sec. V.

On the technical side, this paper is a continuation of the program of Gelfand and Lu^{9,10} to calculate electronic properties of the A_3C_{60} compounds through the direct application of the Kubo-Greenwood formula to tight-binding models for the conduction-band states through exact diagonalization of finite systems. We have extended those calculations in two ways: first, we have extended the usual Kubo-Greenwood formalism to nonzero magnetic field and implemented calculations of $d\sigma_{xy}(B)/dB|_{B=0}$ (the first-order correction to the Hall conductance σ_{xy} , which we denote σ'_{xy}), and second, we have extended the tight-binding models to include Anderson-type disorder.

II. TIGHT-BINDING MODELS FOR A_3C_{60}

In building tight-binding models for the conduction-band states of A_3C_{60} phases, we started with the class of models constructed by Gelfand and Lu^{9,10} using simple Hckel theory. These models are characterized by a set of 3×3 matrices that contain the intermolecular transfer-matrix elements for the t_{1u} orbitals, and that depend on the relative position and orientation of nearest-neighbor molecules. Those matrix elements can, alternatively, be extracted from *ab initio* electronic structure calculations, as was done by Erwin and Mele.¹⁶ Regardless of the source of the matrix elements, in writing down such a model we are assuming that the conduction-band states are derived almost exclusively from the lowest unoccupied molecular orbitals. All of the calculations reported below used the Gelfand and Lu matrix elements; however, we did carry out a subset of them using the Erwin and Mele matrix elements and found no substantial differences.

Within the tight-binding models, merohedral disorder is

accounted for exactly by generating finite clusters, with the molecular orientations drawn from a suitable distribution. In order to minimize the parameter space of our explorations, and in the absence of precise experimental knowledge concerning orientational correlations in the materials, we considered only two types of orientational distributions: fully ordered, corresponding to the $Fm\bar{3}$ crystal structure assumed in most *ab initio* calculations, and uncorrelated random, with each molecule taking either of the two low-energy orientations with equal probability independently of the orientations of its neighbors. The fully ordered systems are not experimentally realizable, but we initially included them because they permitted tests of Matthiessen's rule, they made possible an exploration of the effects of different types of disorder with similar strengths (as evidenced by σ_{xx}) on the Hall coefficient, and they enabled a comparison with a calculation of Erwin and Pickett¹⁷ of the Hall coefficient in orientationally ordered A_3C_{60} structures as a function of band filling. To clarify the last remark, the *ab initio* density-functional calculations all imply a half-filled conduction band, but one can take the band dispersions for such systems and then vary the electron count by hand, assuming rigid bands. Thus one can determine the Fermi surfaces "as a function of band filling," and with some further assumptions evaluate R_H . Hence one of the parameters in the calculations presented below is the band filling F , even though when we began this work had no reason to expect values other than $F = 1/2$ to be relevant to the actual materials.

To account for other kinds of disorder which can exist in these materials we employ a model which introduces only one additional parameter: uncorrelated Anderson disorder with a common value for the three orbitals associated with each molecule. Although this is hardly a realistic model for any kind of disorder in the A_3C_{60} materials (for example, alkali vacancies would certainly lead to short-range correlations between shifts in molecular-orbital energies, as well as break the symmetry responsible for the threefold degeneracy of the t_{1u} orbitals) it should be sufficient to test the hypothesis of Lu *et al.*

To summarize, the models we will study have the form

$$H = \sum_{(i\mu)(j\nu)} t_{(i\mu)(j\nu)} c_{i\mu}^\dagger c_{j\nu} + \sum_{i\mu} V_i c_{i\mu}^\dagger c_{i\mu}, \quad (1)$$

where i and j are indices that run over the C_{60} molecules, and μ and ν are molecular-orbital indices. Merohedral disorder is manifested in the implicit dependence of $t_{(i\mu)(j\nu)}$ on the orientations of molecules i and j and on their relative position. The second term in Eq. (1) is the Anderson disorder, with the V_i distributed uniformly on $[-D/2, D/2]$, and we will refer to D as the strength of the Anderson disorder. We will use the following nomenclature in referring to these models: "Anderson systems" are fully orientationally ordered, and the special case $D = 0$ will be denoted a "clean system." "Mixed systems" are merohedrally disordered, and the special case $D = 0$ will be denoted a "merohedral system."

Magnetic fields are introduced via the London-Peierls approximation,¹⁸ in which the zero-field matrix elements are modified by phase factors:

$$t_{(i\mu)(j\nu)} = t_{(i\mu)(j\nu)}^0 e^{i\Theta_{ij}}$$

$$\Theta_{ij} = \frac{\pi}{\Phi_0} (\mathbf{A}_i - \mathbf{A}_j) \cdot (\mathbf{R}_i + \mathbf{R}_j), \quad (2)$$

where \mathbf{R}_i is the center of molecule i , \mathbf{A}_i is the vector potential at \mathbf{R}_i , and the superscript on t^0 indicates the zero-field value. For the purposes of the Hall effect calculations we take a magnetic field in the z direction, for which $\mathbf{A} = Bx\hat{y}$ (with B the magnetic-field strength) is a convenient gauge choice.

There is also an effect of magnetic field on the molecular orbitals themselves. The t_{1u} orbitals can be represented by states that are symmetric with respect to 180° rotation about x , y , and z . The magnetic field has no effect on the z -symmetric state, but mixes the x - and y -symmetric states. Within the usual Hückel theory for the C_{60} molecule (following, for example, Elser and Haddon,¹⁹ and taking 1.2 as the ratio of matrix elements for short versus long bonds) one finds low-field matrix elements $t_{(ix)(iy)} = -iB 1.75 \times 10^{-3}$ eV/T, which are roughly a factor of 10 smaller than the other imaginary terms in the Hamiltonian associated with the intermolecular matrix elements. We found that neglecting these intramolecular matrix elements typically leads to 10% or less effects on the transverse conductivity; in fact we did almost all calculations both with and without them, and found that whether or not they were included had no effect on our conclusions. Since including the intramolecular matrix elements introduces a third energy scale into the problem, in addition to the scales of t^0 and D , for simplicity we will present here the results for calculations in which those matrix elements are ignored.

Finally, within the tight-binding formalism, note that current operators are simply expressed in terms of matrix elements of the Hamiltonian:

$$\mathbf{j}_{(i\mu)(j\nu)} = \frac{ie}{\hbar} t_{(i\mu)(j\nu)} (\mathbf{R}_i - \mathbf{R}_j). \quad (3)$$

III. FINITE-CLUSTER KUBO-GREENWOOD METHOD

Various approaches, all based ultimately on the Kubo-Greenwood formula, have been used to numerically evaluate elements of the conductivity tensor in tight-binding models. Examples include transfer-matrix methods^{20,21} and various forms of the recursion method.^{22,23} Using these approaches, calculations of off-diagonal elements of σ are rare, and we are aware of only two references: Houari and Harris²⁴ and Czycholl.²⁵

Our procedure is of a different nature, as we apply the Kubo-Greenwood equation directly to finite systems. The use of finite-cluster methods for density of states and longitudinal conductivity has ample precedent and does not require much discussion. The Hall effect is another matter. For a magnetic field along the z axis, the low-field Hall coefficient

can be expressed in terms of the conductivity tensor as $R_H = \sigma'_{xy}/\sigma_{xx}^2$, with $\sigma'_{xy} \equiv d\sigma_{xy}/dB|_{B=0}$. We know of no other calculation of σ'_{xy} by direct evaluation on finite clusters, so it is appropriate to discuss some technical aspects of both the finite-cluster calculations themselves and the various extrapolations required to obtain values that can be compared with experimental data on macroscopic samples.

One potential benefit of our approach is that the frequency dependent σ_{xx} and σ'_{xy} (or at least the intraband contribution thereto) are obtained, not just the dc values. However, for the relevant frequency range in A_3C_{60} experiments are rarely carried out for the transverse conductivity because they are technically difficult.²⁶

A. Formalism and boundary conditions

In three dimensions, the $T=0$ Kubo-Greenwood formula can be written in the form

$$\sigma_{\alpha\beta}(\omega) = \frac{e^2}{\hat{a}h} \frac{4\pi}{\omega V} \lim_{\eta \rightarrow 0^+} \sum_{\epsilon_n < \epsilon_F < \epsilon_m} \langle n | j_\alpha | m \rangle \times \langle m | j_\beta | n \rangle \frac{-i}{\omega + \epsilon_n - \epsilon_m + i\eta}. \quad (4)$$

Here we have introduced a length scale \hat{a} and an energy scale $\hat{\epsilon}$, redefined the angular frequency $\hbar\omega/\hat{\epsilon} \rightarrow \omega$, and pulled out all factors of the energy and length scales, as well as all the prefactors from the current operators, so that every quantity to the right of the first fraction is individually dimensionless. We take \hat{a} to be half the conventional fcc lattice constant, so that the \mathbf{R}_i have integer Cartesian coordinates; then V is eight times the number of conventional unit cells in the cluster. For an A_3C_{60} fcc lattice constant of 14.4 \AA , $e^2/\hat{a}h = 536 (\Omega \text{ cm})^{-1}$, which we will adopt below whenever it is appropriate to produce numbers that can be compared with experiment. The energy scale does not enter into the dc conductivity at all. We will take $\hat{\epsilon}$ to be the bandwidth of a ‘‘merohedral system’’ (roughly 0.5 eV), and we will quote all energies in terms of this unit. The London-Peierls phase factors into a dimensionless magnetic-field strength $b = B\hat{a}^2/\Phi_0$ and a geometric part $\theta_{ij} = \pi(x_i - x_j)(y_i + y_j)$.

Boundary conditions on the clusters cannot be chosen arbitrarily. Periodic boundary conditions are generally used for finite-cluster calculations because they minimize finite-size effects. However, periodic lattice boundary conditions are impossible to satisfy for arbitrary values of b ; the allowed values are given (for our choice of gauge) by $b = q/N_y$ where q is an integer and N_y is the number of unit cells in the \hat{y} direction. For a typical calculation on a $6 \times 6 \times 4$ lattice the minimum allowed value of B amounts to roughly 400 T. Czycholl²⁵ used periodic boundaries and proceeded in this fashion; however, that calculation was explicitly high field. Since we are instead interested in the low-field Hall effect, we will employ open boundaries along x and y and periodic

boundary conditions only along z . Notwithstanding the periodicity in z , we will refer to these as “open” boundary conditions.

Calculations of the conductivity may be carried out for any magnetic-field strength with these boundary conditions, but we will go one step further and expand the Kubo-Greenwood formula itself to first order in the magnetic field to obtain an expression for σ'_{xy} . There are several advantages to doing so, rather than evaluating σ_{xy} itself at nonzero b . In the formula for σ'_{xy} all numerical calculations can be done with real numbers, while complex numbers are needed for σ_{xy} . For finite clusters, $\sigma_{xy}(b=0) \neq 0$ except for realizations of disorder which by rare chance are invariant under $\pi/2$ rotation about the z axis; hence to determine σ'_{xy} for even a single cluster requires either a calculation at two fields or calculations of both σ_{xy} and σ_{yx} , and in either case one has to check that b is small enough to be in the linear regime but sufficiently large that the finite precision of numerical calculations is not distorting the results.

Expanding the Kubo-Greenwood formula to first order in b requires expanding the current operators and the eigenfunctions to first order. The eigenvalues have no first-order correction except for the Zeeman effect, which affects all states of a given spin equally and gives no contribution to the conductivity and so is not even included in the model, Eq. (1).

The first-order corrections to the Hamiltonian and current matrices are $ibt'_{(i\mu)(j\nu)} = ib\theta_{ij}t'_{(i\mu)(j\nu)}$ and $ib\mathbf{j}'_{(i\mu)(j\nu)} = ib\theta_{ij}\mathbf{j}_{(i\mu)(j\nu)}$, respectively. The first-order correction to the eigenstate $|a\rangle$ can be written as the usual result from perturbation theory, $ib|a'\rangle = ib\sum_{m \neq a} |m\rangle \langle m|t'|a\rangle / (\epsilon_a - \epsilon_m)$.

The expansions for the current operators and eigenfunctions are then inserted into the matrix elements appearing in Eq. (4) and only terms of first order retained. The product of matrix elements then has six terms, $ib\langle n^0|j_x^0|m^0\rangle \langle m^0|j_y^0|n'\rangle$ and so forth, with superscript zeros again denoting zero-field values. The resulting expression for σ'_{xy} requires roughly ten times more computational effort than that for the zero field σ_{xx} .

B. Extrapolations to dc and thermodynamic limits

For both σ_{xx} and σ'_{xy} , calculations on finite samples must be appropriately extrapolated in order to obtain results which can be compared with data on macroscopic samples.

Since we are considering disordered systems we average over realizations of the disorder. Ten to one hundred realizations are typically used, and the sample-to-sample variations lead to the statistical uncertainties in the results quoted below.

The $\eta \rightarrow 0$ limit in the Kubo-Greenwood formula cannot be taken literally in finite systems, since that leads to a set of discrete δ functions (for σ_{xx}) or poles (for σ'_{xy}) rather than smooth distributions. Instead, one can evaluate the conductivity at some frequency as a function of η . For η sufficiently larger than the spacing between transition energies the behavior is smooth, and that can be extrapolated to $\eta = 0$. In such extrapolations one should not take into account data for η so large that it is comparable to physical energy

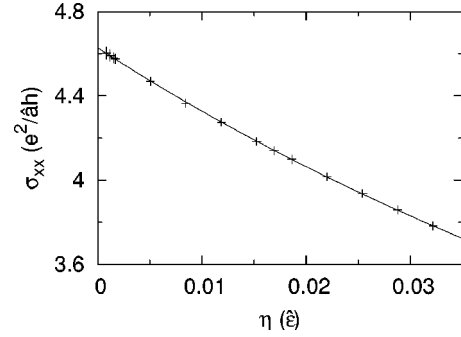


FIG. 1. Example of fitting $\sigma_{xx}(\eta)$ data to $1/(p\eta + q)$. These data are for a mixed system with $D=0.169$ and $F=0.5$.

scales such as the inverse relaxation time, but as there are typically several decades between the lower and upper limits this can be arranged.

For clusters with periodic boundary conditions, σ_{xx} has a maximum at $\omega = 0$; however, for the boundary conditions we employ its maximum is at some other frequency which has some sample-to-sample variation but is primarily size dependent. We will always take the values at the lowest-frequency peaks of the ensemble-averaged data in both σ_{xx} and σ'_{xy} (the frequencies of which track each other nicely) for the “dc” value.

Finally, there is the matter of extrapolating the results as a function of system size, which in principle ought to be done but, as will be seen, has been neglected. Unless otherwise stated, results shown below are for $6 \times 6 \times 4$ systems, which have 1728 orbitals.

All of the various extrapolations, and other assumptions in the data analysis, together lead to the “procedural” uncertainties that are quoted subsequently. These can only be roughly estimated, so we have tried to be conservative. They are typically about twice the statistical uncertainties.

Let us present here some concrete results to illustrate the extrapolation procedures and other assumptions.

C. Extrapolating η to 0

Figure 1 shows an example of fitting σ_{xx} as a function of η using the form $1/(p\eta + q)$. This two-parameter fit for the low-frequency peak value of σ_{xx} was adopted for all extrapolations in η . It works well, and it has the appropriate large- η behavior. However, simple least-squares fitting procedures do not lead to appropriate error estimates for the fit parameters. Weighting all points equally usually gives an excellent fit, leading to error estimates in the fit parameters that are too small, in the sense that modestly changing the range of η over which to fit leads to much larger variation in those parameters. Weighting points according to their statistical errors is also unsatisfactory, as that tends to underweight the smaller- η data, which should have more *a priori* significance than the larger- η data. In the end, we used unweighted fits and examined the variation in the fit parameters with the η range included in the fit. We always assigned at least a 5% procedural error to the fitting procedure.

For σ'_{xy} , one expects $\sigma'_{xy} \sim \eta^{-2}$ at large η . That indeed holds in our data, but there are several reasonable choices for

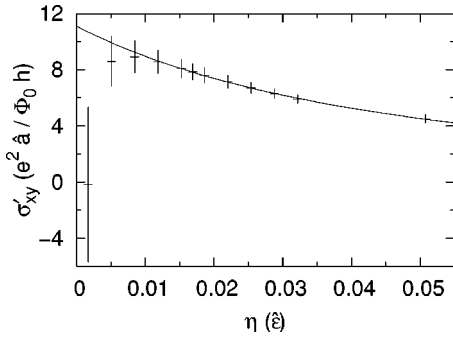


FIG. 2. Example of fitting $\sigma'_{xy}(\eta)$ to $1/(p\eta+q)^2$. This is a merohedral system with $F=0.6$.

fitting functions for σ'_{xy} —we considered $1/(p\eta^2+q)$, $1/(p\eta^2+q\eta+r)$, and $1/(p\eta+q)^2$ —none of which works as well as the fit to σ_{xx} . We settled on $1/(p\eta+q)^2$ (see Fig. 2), but note that the range of η that can be used in the fits for σ'_{xy} is narrower than for σ_{xx} , and there are greater associated procedural errors. Figure 2 also demonstrates the necessity of deciding which values of η are useful: too small and the results are not physically meaningful. Uncertainties in this judgement as well as the statistical uncertainty in σ'_{xy} (greater than in σ_{xx}) lead us to be more conservative, and report at least a 7% error in the results of $\lim_{\eta \rightarrow 0^+} \sigma'_{xy}$.

D. Boundary condition and finite-size effects

For periodic systems, the finite-size effects in the conductivity for merohedrally disordered A_3C_{60} are known to be quite small. For example, periodic $4 \times 4 \times 4$ and $6 \times 6 \times 6$ systems yield almost indistinguishable results for σ_{xx} .¹⁰ However, data for σ'_{xy} are only available for systems with open boundary conditions, for which one might anticipate stronger finite-size effects. To gauge the finite-size and boundary effects, in Fig. 3 we compare the results for the longitudinal conductivity in open and periodic merohedral system at various band fillings. It appears that the open boundaries lead to a systematic underestimate of about 20%, but the dependence on F is captured correctly. In Fig. 4, the difference between the two boundary conditions is illustrated in more detail by plotting the frequency dependence of σ_{xx} at one particular value of F . As one would expect, away from $\omega=0$ the curves are hardly distinguishable. With open

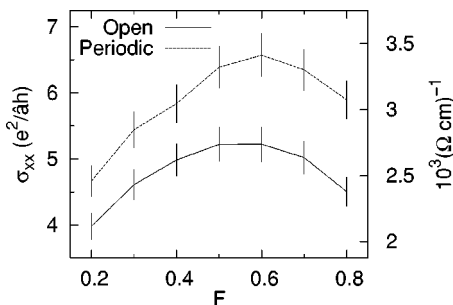


FIG. 3. Extrapolated ($\eta \rightarrow 0$) σ_{xx} as a function of band filling, for $6 \times 6 \times 4$ merohedral systems with periodic and open boundaries.

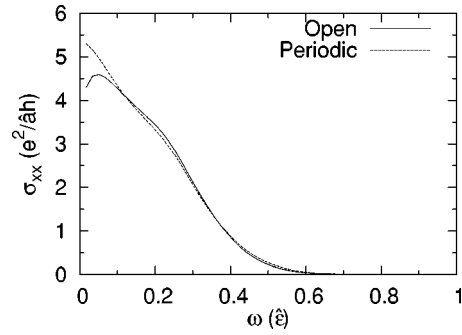


FIG. 4. $\sigma_{xx}(\omega)$ for merohedral systems at half filling with open and periodic boundary conditions. Here we set $\eta=0.01$, rather than carrying out $\eta \rightarrow 0$ extrapolations at every value of ω . Statistical errors are roughly the width of the lines.

boundaries the maximum in the Drude peak is pushed to a finite frequency, and so the value at the maximum is less than for periodic boundaries.

It is impossible to carry out a similar comparison for σ'_{xy} . However, considering the plots of $\sigma'_{xy}(\omega)$ shown in Fig. 5, it seems likely that open boundaries would again lead to systematic underestimates in the magnitude of the quantity, and thus the systematic errors associated with open boundaries may partially cancel in evaluating R_H .

E. Validation of the Hall effect calculation for the square-lattice Anderson model

In order to validate our formalism for and implementation of the finite-cluster calculations of σ'_{xy} and R_H , we applied this method to the square lattice, single orbital Anderson impurity model at $2/3$ filling. We considered systems up to 50×50 , and we were careful to find D values (which turned out to be $0.5 \leq D \leq 1$) such that the systems were mesoscopic, since the results for neither localized nor ballistic systems could be sensibly compared with the classical Drude expression for R_H . The results for R_H were in the range 2.5 to $3\hat{a}^2/e$, with roughly 30% uncertainties. (The data for the two-dimensional systems have considerably larger statistical and procedural errors than for the A_3C_{60} models.) This can be compared with the classical Drude result of $1.5\hat{a}^2/e$, and with the value $0.989a^2/e$ which was derived from Ong's construction²⁷ together with the assumption that the scattering rate is constant over the Fermi surface. We consider the

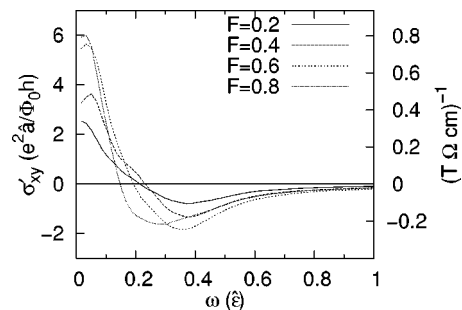


FIG. 5. $\sigma'_{xy}(\omega)$ for merohedral systems at several band fillings. Here, $\eta=0.032$. Statistical error bars are omitted for clarity.

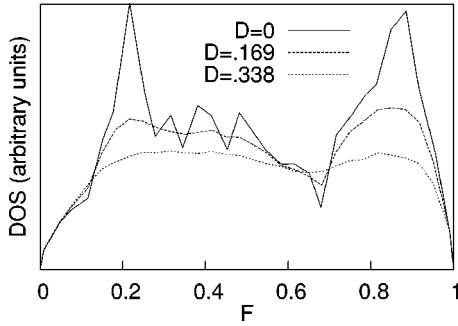


FIG. 6. Density of states as a function of band filling for Anderson systems.

agreement acceptable, and believe that the differences can be ascribed to shortcomings of the latter theoretical approaches.

IV. RESULTS

A. Density of states

The density of states (DOS) can give one a rough idea of the effect of disorder on electronic states, as detailed structure present in the DOS for clean systems will become washed out as disorder is introduced. We will present plots of DOS as a function of band filling F rather than as a function of energy, so the areas under DOS curves should not be equal. Since the actual value of the DOS coming out of these calculations is not of particular interest (it will scale as $\hat{\epsilon}^{-1}$), the graphs will just show “arbitrary units” on the ordinate.

The DOS for some Anderson and mixed systems are shown in Figs. 6 and 7, respectively. It is worth noting that while Anderson disorder at the strengths considered here largely washes out the prominent features in the clean-system DOS, adding Anderson disorder to a system with merohedral disorder already present has hardly any effect at all on the shape of the DOS curve. The main effect of Anderson disorder in the latter case is to broaden the band; Fig. 8 shows how the bandwidth (which is $1\hat{\epsilon}$, by definition, for a merohedral system) depends on D for both Anderson and mixed systems.

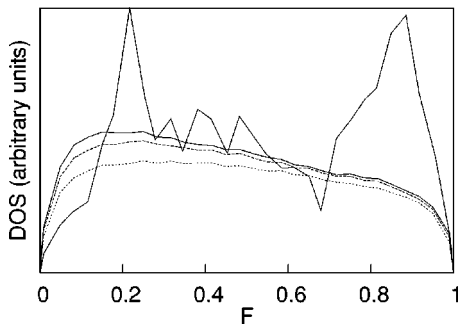


FIG. 7. Density of states as a function of band filling for several mixed systems: $D=0$ (solid), $D=0.169$ (dashed), and $D=0.338$ (dotted). The clean-system DOS (from Fig. 6) is shown for comparison as a solid line.

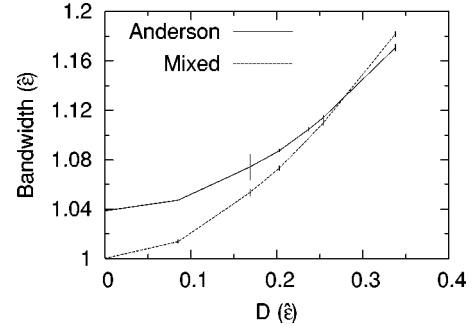


FIG. 8. Bandwidth as a function of disorder parameter D for both Anderson and mixed systems.

B. Longitudinal conductivity and Matthiessen’s rule

The longitudinal conductivity is a necessary ingredient in the calculation of R_H , and there are some interesting results for the models we have explored. First, inspection of Figs. 3 and 7 reveals that the conductivity in merohedral systems is increasing over an interval in band filling where the density of states is decreasing slightly. This is not completely surprising, as one does not expect the conductivity to be simply proportional to the DOS since the scattering intensity can depend on F as well, but it is a hint of things to come.

Let us now turn to Anderson systems. The corresponding results for conductivity as a function of band filling, for several D values, are given in Fig. 9. We were interested in finding a value of D which would give an Anderson system with nearly the same conductivity as a merohedral system, so that one could compare the effects of two distinct types of disorder of the same “strength” on R_H , and apparently $D \approx 0.2$ is appropriate, at least for $F \approx 1/2$. For the less strongly disordered systems there is a dip in σ_{xx} for $F \approx 2/3$, corresponding to the location of the minimum in the DOS. One would expect that $\sigma_{xx} \sim 1/D$ in these systems. That holds quite well except for the smallest value of D , where the conductivity seems to be too small. This can be attributed to the finite size and open boundary conditions: as D is reduced eventually the mean free path becomes comparable to the system size, and the width of the Drude peak is no longer much greater than the finite-size induced peak frequency in $\sigma_{xx}(\omega)$.

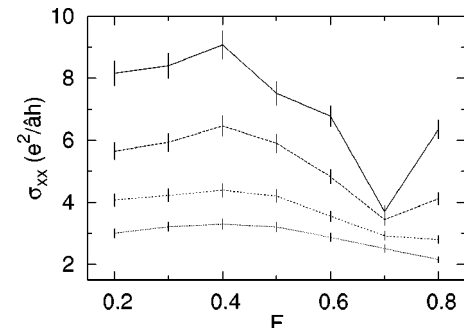


FIG. 9. σ_{xx} as a function of band filling for Anderson systems. The curves are for disorder strengths $D=0.085$, 0.169 , 0.253 , and 0.338 , from top to bottom.

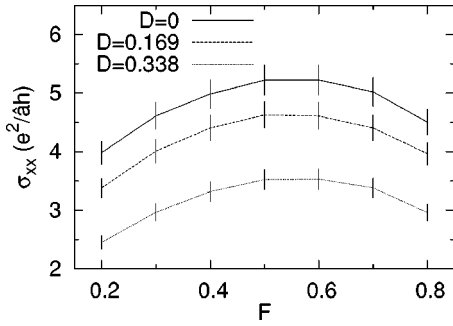


FIG. 10. σ_{xx} as a function of band filling for mixed systems.

Finally, we present the results for mixed systems. The plots of conductivity as a function of filling, Fig. 10, are similar to the merohedral case.

Since the models have two types of disorder, an obvious question follows: does Matthiessen’s rule hold? Figure 11 shows that it does not, at least for the value of D at which the two types of disorder are roughly the same strength. The violation of Matthiessen’s rule is quite striking. The deviation from Matthiessen’s rule shown in the figure is $\Delta\rho = \rho_{\text{mero}} + \rho_{\text{And}} - \rho_{\text{mixed}}$; expressed as a fraction of ρ_{mixed} , this is never less than 50% in the plot. In fact, the resistivity in mixed systems is, for the larger fillings, actually *less* than the resistivity for the corresponding Anderson systems, corresponding to a fractional violation greater than 100%. Such a reduction in resistivity with additional disorder takes place at half filling for sufficiently large D , as seen in Fig. 12. The significance of such grossly nonadditive resistivities will be discussed in the conclusions.

C. Transverse conductivity and Hall coefficient

For merohedral systems, the results of the calculations and extrapolations for σ'_{xy} and R_H are given in Figs. 13 and 14, respectively. Note, most prominently, that there is no sign change as a function of band filling. This stands in contrast to Fig. 2 from Erwin and Pickett,¹⁷ which shows a sign change near half filling in addition to other obvious structure in R_H

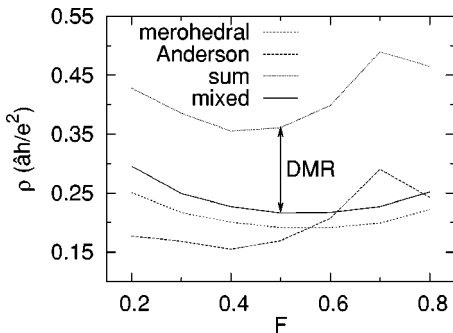


FIG. 11. Resistivity as a function of band filling for Anderson, merohedral, and mixed systems. The disorder parameter for Anderson and mixed systems is $D=0.169$. Error bars are omitted for clarity. Also plotted is the sum of the merohedral and Anderson resistivities. The difference between the sum curve and the mixed system curve is the deviation from Matthiessen’s rule, labeled DMR.

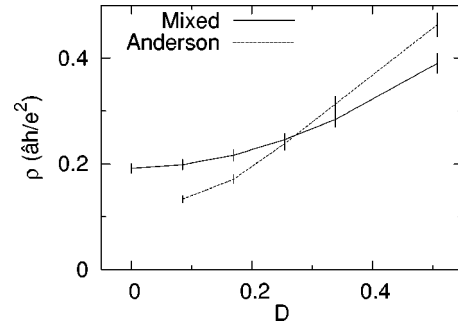


FIG. 12. Resistivity as a function of Anderson disorder strength for mixed and Anderson systems at half filling. Deviations from Matthiessen’s rule are evident in that the curves are not simply displaced vertically with respect to each other. As noted in the text, the resistivity for the cleanest Anderson system shown is likely an overestimate.

as a function of Fermi energy. These differences may not be too surprising, considering how much the DOS differs between Anderson and merohedral systems, but it certainly violates the conventional wisdom that disorder only weakly influences the low-field Hall effect. In contrast, the Hall coefficient in Anderson systems (see Fig. 15) does exhibit a sign change as a function of band filling. The value at half filling for low disorder, $R_H = (5.6 \pm 0.9) \times 10^{-9} \text{ m}^3/\text{C}$, may be compared with Erwin and Pickett’s¹⁷ result $7.0 \times 10^{-9} \text{ m}^3/\text{C}$. With increasing disorder strength, one finds only a weak dependence until D exceeds 0.4, at which point R_H seems to rapidly decrease. This may reflect localization at strong Anderson disorder; we did not investigate this regime closely.

Finally, we turn to the calculations for mixed systems, which are most directly related to the original motivation for this work. Figure 14 shows the dependences of R_H on filling for two mixed systems. They are similar to the merohedral case, and show little of the structure seen in Anderson systems. The critical test of the hypothesis of Lu *et al.* is presented in Fig. 16, which shows the Hall coefficient at half filling as a function of Anderson disorder strength. There is little variation in R_H , and certainly no sign change, even up to $D \approx (2/3)\hat{e}$.

V. CONCLUSIONS

The deviations from Matthiessen’s rule seen in alkali metals have led to some difficulty in the interpretation of low-

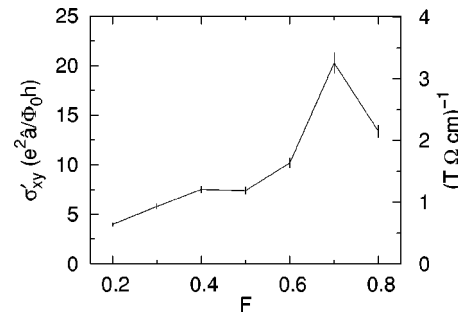


FIG. 13. σ'_{xy} as a function of band filling for merohedral systems.

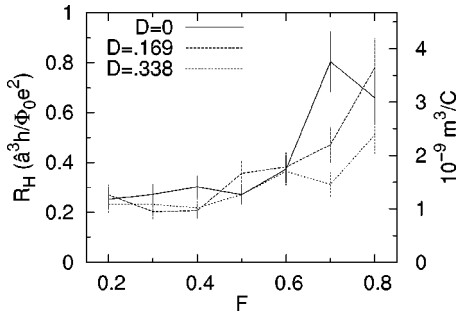


FIG. 14. Hall coefficient for merohedral ($D=0$) and mixed systems as a function of band filling.

temperature conductivity data²⁸ in those materials. The enormous violations of Matthiessen's rule evident in the present calculations suggest that caution should be applied in the interpretation of conductivity data in A_3C_{60} systems. While extracting the electron-phonon coupling from high-temperature resistivity data (as in Ref. 11) is probably safe, since the residual resistivity is rather small compared to the high-temperature resistivity, extracting quantitative information from the low-temperature T^2 behavior (as in Refs. 29 and 30) may be more perilous.

Regarding the Hall effect, our results do not support the hypothesis presented by Lu *et al.*¹³ to account for the observed variation of the Hall conductance with lattice spacing in A_3C_{60} systems. At half filling we find R_H to be positive at low D (corresponding to small lattice constant) in mixed systems, and with increasing D (increasing lattice constant) our calculations suggest no variation at all of R_H with D . It is simply not the case that a generic model containing merohedral disorder and some other kind of disorder will exhibit the experimentally observed variations in R_H as the strength of the latter is varied.

How, then, to account for the discrepancies between our calculations and the behavior observed experimentally by Lu *et al.*? In other words, why does R_H behave as it does in K_3C_{60} and Rb_3C_{60} ? There are several possibilities to consider.

First, the basic idea of Lu *et al.* might be correct, except that the variation of R_H does not hold for *generic* disorder which has strength increasing (relative to the bandwidth) with a . Perhaps simple Anderson disorder lacks some crucial

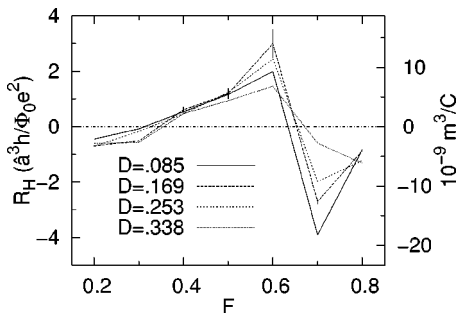


FIG. 15. Hall coefficient as a function of band filling for Anderson systems with several values of D . Error bars are only shown for $D=0.169$, and are barely visible except for $F=0.4, 0.5, 0.6$.

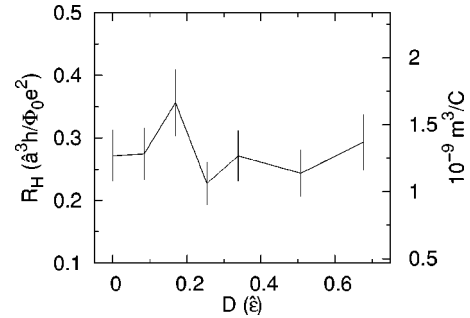


FIG. 16. Hall coefficient for mixed systems at half filling as a function of Anderson disorder parameter D .

property of the nonmerohedral disorder that is present in A_3C_{60} samples. This seems unlikely to us. It must be admitted, however, that we have found that R_H can have a strong dependence on the type of disorder that is present: compare Figs. 14 and 15. Merohedral disorder is apparently strong in terms of its effects on the Hall coefficient, in a way that Anderson disorder is not. This leads to another idea: perhaps our treatment of orientational disorder is inadequate. We considered only uncorrelated merohedral disorder, but there are theoretical analyses^{31,32} and experimental results³³ which suggest that there are correlations between orientations of neighboring molecules, and that they tend to have different orientations rather than the same one. It seems plausible that the degree of orientational correlations would have a marked effect on R_H , but it is not obvious that there should be a universal relationship between the lattice constant and the orientational correlations. This issue merits further exploration.

Second, perhaps the assumption that the R_H versus a curve reflects $T=0$ physics is faulty. This seems unlikely. Even at 50 K there is a substantial difference in R_H between K_3C_{60} and Rb_3C_{60} , and there is no good reason to attribute the observed behavior to thermal effects.

Third, other physics may be contributing in some fashion to the Hall effect. Given their narrow conduction bandwidths, the A_3C_{60} materials cannot be very far from a Mott transition with increasing a (see Sec. IV of Gunnarsson's review³⁴), although as long as they are "ordinary metals" the analysis of Schulz and Allen¹⁵ suggests that the electron-electron interactions should not significantly change R_H . More dramatic effects of electron-electron and electron-phonon interactions, such as the intramolecular charge disproportionation proposed by Ceulemans, Chibotaru, and Cimpoesu,³⁵ might account for the experimental R_H versus a curve but the mechanism for such is hardly clear. Let us just say that the experimental results of Lu *et al.* offer a challenge to every theory of the low-energy electronic properties of the A_3C_{60} materials.

Finally, let us make some observations concerning the experimental results, our theoretical calculations, and one electronic structure calculation which are suggestive, but do not quite constitute an explanation of the data. It seems to be impossible to account for the experimental results in models containing uncorrelated merohedral disorder, with or without Anderson disorder: varying either D or F (the latter being

unphysical, within the usual picture) cannot change the sign of R_H , which remains stubbornly positive, although less in magnitude and much closer to the experimental results at the largest values of a than one obtains for Anderson systems at half filling. However, if one allows F to vary with a , then Anderson systems with F in the range 0.3–0.4 do give the hoped-for results. This is oddly coincidental with an approximate Hartree-Fock calculation by Schulte and Böhm,³⁶ who claim that the net charge transfer from the cations in K_3C_{60} amounts to about 1.5 electrons per molecule (which we might associate with $F=0.25$), and that there is more charge transfer from the octahedral cations (leading one to expect greater charge transfer as a is increased). One cannot take this coincidence at face value. If there really is incomplete charge transfer, then it would be inaccurate to ignore the contribution of the outer alkali s orbitals to the conduction-band states, and one would need to include them on the same footing as the molecular orbitals in a tight-binding model. But suppose, for the sake of argument, that one could ignore the alkali orbitals except for their effect on F —one would also have to worry about the implications of this picture for other electronic properties. At the levels of Anderson disorder which would be needed to account for the residual resistivity, the density of states has little dependence on F in the

relevant range, so the universality of the density of states as a function of lattice constant (and the implications for superconductivity, magnetic resonance, and so on) would hold just as well as in the conventional picture. But it bears repeating that this argument is not based on a consistent model of the electronic structure in A_3C_{60} .

In summary, we have implemented direct evaluation of the Kubo-Greenwood formula on finite-cluster tight-binding models for the low-field transverse conductivity. This method has been applied to a large set of models inspired by the A_3C_{60} materials. We have found that the interplay of Anderson disorder and merohedral disorder is, by itself, unable to account for the remarkable experimental results of Lu *et al.* concerning the Hall coefficient in K_3C_{60} and Rb_3C_{60} . We have also encountered enormous deviations from Matthiessen's rule, which may confound the analysis of the temperature dependence of the conductivity in these materials.

ACKNOWLEDGMENTS

We would like to thank V. Crespi and S. Sondhi for correspondence and conversations. This work was supported by the National Science Foundation through Grant No. DMR 94-57928.

-
- ¹R.C. Haddon, A.F. Hebard, M.J. Rosseinsky, D.E. Murphy, S.J. Duclos, K.B. Lyons, B. Miller, J. Rosamilia, R.M. Fleming, and A.R. Kortan, *Nature (London)* **350**, 320 (1991).
- ²A.F. Hebard, M.J. Rosseinsky, R.C. Haddon, D.W. Murphy, S.H. Glarum, T.T.M. Palstra, A.P. Ramirez, and A.R. Kortan, *Nature (London)* **350**, 600 (1991).
- ³M.J. Rosseinsky, A.P. Ramirez, S.H. Glarum, D.W. Murphy, R.C. Haddon, A.F. Hebard, T.T.M. Palstra, A.R. Kortan, S.M. Zahurak, and A.V. Makhija, *Phys. Rev. Lett.* **66**, 2830 (1991).
- ⁴J.L. Martins and N. Troullier, *Phys. Rev. B* **46**, 1766 (1992).
- ⁵S. Satpathy, V.P. Antropov, O.K. Andersen, O. Jepsen, O. Gunnarsson, and A.I. Liechtenstein, *Phys. Rev. B* **46**, 1773 (1992).
- ⁶R.C. Haddon, *Acc. Chem. Res.* **25**, 127 (1992).
- ⁷P.W. Stephens, L. Mihaly, P.L. Lee, R.L. Whetten, S.-M. Hwang, R. Kaner, F. Deiderich, and K. Holczer, *Nature (London)* **351**, 632 (1991).
- ⁸P.W. Stephens, L. Mihaly, J.B. Wiley, S.-M. Hwang, R. Kaner, F. Deiderich, R.L. Whetten, and K. Holczer, *Phys. Rev. B* **45**, 543 (1992).
- ⁹M.P. Gelfand and J.P. Lu, *Phys. Rev. Lett.* **68**, 1050 (1992).
- ¹⁰M.P. Gelfand and J.P. Lu, *Phys. Rev. B* **46**, 4367 (1992).
- ¹¹J.G. Hou, L. Lu, V.H. Crespi, X.-D. Xiang, A. Zettl, and M.L. Cohen, *Solid State Commun.* **93**, 973 (1995).
- ¹²J.E. Fischer, G. Bendele, R. Dinnebier, P.W. Stephens, C.N. Lin, N. Bykovetz, and Q. Zhu, *J. Phys. Chem. Solids* **56**, 1445 (1995).
- ¹³L. Lu, V.H. Crespi, M.S. Fuhrer, A. Zettl, and M.L. Cohen, *Phys. Rev. Lett.* **74**, 1637 (1995).
- ¹⁴T.T.M. Palstra, R.C. Haddon, A.F. Hebard, and J. Zaanen, *Phys. Rev. Lett.* **68**, 1054 (1992).
- ¹⁵W.W. Schulz and P.B. Allen, *Phys. Rev. B* **52**, 7994 (1995).
- ¹⁶S.C. Erwin and E.L. Mele, *Phys. Rev. B* **50**, 5689 (1994).
- ¹⁷S.C. Erwin and W.E. Pickett, *Phys. Rev. B* **46**, 14 257 (1992).
- ¹⁸J.A. Pople, *J. Chem. Phys.* **37**, 53 (1962).
- ¹⁹V. Elser and R.C. Haddon, *Nature (London)* **325**, 792 (1987).
- ²⁰A. MacKinnon, *J. Phys. C* **13**, 1031 (1980).
- ²¹N. Giordano, *Phys. Rev. B* **36**, 4190 (1987).
- ²²D. Mayou, *Europhys. Lett.* **6**, 549 (1988).
- ²³L.E. Ballentine and J.E. Hammerberg, *Can. J. Phys.* **62**, 692 (1984).
- ²⁴A. Houari and R. Harris, *J. Phys.: Condens. Matter* **4**, 1505 (1991).
- ²⁵G. Czycholl, *Solid State Commun.* **67**, 499 (1988).
- ²⁶S.G. Kaplan, S. Wu, H.-T.S. Lihn, H.D. Drew, Q. Li, D.B. Fenner, J.M. Phillips, and S.Y. Hou, *Phys. Rev. Lett.* **76**, 696 (1996).
- ²⁷N.P. Ong, *Phys. Rev. B* **43**, 193 (1991).
- ²⁸J. Bass, W.P. Pratt, Jr., and P.A. Schroeder, *Rev. Mod. Phys.* **62**, 645 (1990).
- ²⁹T.T.M. Palstra, A.F. Hebard, R.C. Haddon, and P.B. Littlewood, *Phys. Rev. B* **50**, 3462 (1994).
- ³⁰V.H. Crespi and M.L. Cohen, *Phys. Rev. B* **52**, 3619 (1995).
- ³¹I.I. Mazin, A.I. Liechtenstein, O. Gunnarsson, O.K. Andersen, V.P. Antropov, and S.E. Burkov, *Phys. Rev. Lett.* **70**, 4142 (1993).
- ³²T. Yildirim, S. Hong, A.B. Harris, and E.J. Mele, *Phys. Rev. B* **48**, 12 262 (1993).
- ³³S. Teslic, T. Egami, and J.E. Fischer, *Phys. Rev. B* **51**, 5973 (1995).
- ³⁴O. Gunnarsson, *Rev. Mod. Phys.* **69**, 575 (1997).
- ³⁵A. Ceulemans, L.F. Chibotaru, and F. Cimpoesu, *Phys. Rev. Lett.* **78**, 3725 (1997).
- ³⁶J. Schulte and M.C. Böhm, *Solid State Commun.* **93**, 249 (1995).